Title

Clinical description with magnetic resonance appearance of a high-grade undefined optic nerve glioma with intracranial extension.

Permalink

https://escholarship.org/uc/item/4t04q670

Journal

The Canadian veterinary journal. La revue veterinaire canadienne, 64(8)

ISSN

0008-5286

Authors

Charnock, Lauren

Jukier, Tom

Shaw, Gillian

et al.

Publication Date

2023-08-01

Peer reviewed

Case Report Rapport de cas

Clinical description with magnetic resonance appearance of a high-grade undefined optic nerve glioma with intracranial extension

Lauren N. Charnock, Tom Jukier, Gillian C. Shaw, Alana Kramer, Emily Brinker, Phillip A. Moore

Abstract — A 4-year-old mixed-breed dog was presented for hyphema and glaucoma of the right eye. Enucleation of the right globe was carried out, and histopathology examination revealed an optic nerve glioma with incomplete surgical margins. At 8 wk after surgery, the dog had depressed mentation and a diminished pupillary light reflex of the left eye. Magnetic resonance imaging revealed an irregular, heterogeneously T2 hyperintense/T1 isointense mass in the region of the optic chiasm. Compression of the rostral thalamus was present, with effacement of the pituitary gland and involvement of the right orbit. The dog was euthanized 4.5 mo after initial presentation. An undefined glioma of the right optic nerve with extension to the diencephalon was diagnosed on necropsy.

Key clinical message:
Although rare, intraocular glioma is a differential diagnosis for hyphema, glaucoma, and retinal detachment. Magnetic resonance imaging should be considered in cases of intraocular neoplasia, notably in those with incomplete surgical margins of the optic nerve.

Résumé — Description clinique avec aspect en résonance magnétique d'un gliome indéfini de haut grade du nerf optique avec extension intracrânienne. Un chien de race croisé âgé de 4 ans a été présenté pour un hyphéma et un glaucome de l'œil droit. Une énucléation du globe droit a été réalisée et l'examen histopathologique a révélé un gliome du nerf optique aux marges chirurgicales incomplètes. Huit semaines après la chirurgie, le chien avait une diminution du processus mental et un réflexe pupillaire à la lumière diminué de l'œil gauche. L'imagerie par résonance magnétique a révélé une masse irrégulière hétérogène hyperintense T2/T1 isointense dans la région du chiasma optique. Une compression du thalamus rostral était présente, avec effacement de l'hypophyse et atteinte de l'orbite droite. Le chien a été euthanasié 4,5 mois après la présentation initiale. Un gliome indéfini du nerf optique droit avec extension au diencéphale a été diagnostiqué à l'autopsie.

Message clinique clé :
Bien que rare, le gliome intraoculaire est un diagnostic différentiel pour l'hyphéma, le glaucome et le décollement de la rétine. L'imagerie par résonance magnétique doit être envisagée en cas de néoplasie intraoculaire, notamment chez ceux dont les marges chirurgicales du nerf optique sont incomplètes.

(Traduit par Dr Serge Messier)

Glial tumors are the second-most common primary brain neoplasm in the dog (after meningiomas) (1) and account for ~1/3 of intracranial neoplasms (1,2). "Glioma" is an encompassing term for several different types of glial cell neoplasia that, in dogs, previously included oligodendroglioma, astrocytoma, oligoastrocytoma, anaplastic gliomas, and glioblastoma multiforme. To help standardize canine glioma classifications, the National Cancer Institute's Comparative Brain Tumor Consortium (CBTC) published a revised classification scheme in 2018 to recategorize glial tumors as either astrocytoma, oligodendroglioma, or undefined glioma based on histopathologic features and immunohistochemistry. An undefined glioma was defined as a glial tumor with < 80% morphology of either astrocytoma or oligodendroglioma (3). Although gliomas may

arise in any portion of the central nervous system, most of these tumors tend to develop in the telencephalon (1), but they have also been diagnosed in the spinal cord (4).

Reports of ocular gliomas in dogs are scarce in the veterinary literature. Potential origins of these tumors include the retinal nerve fiber layer, optic nerve head, and intraorbital portion of the optic nerve (5–12). A retrospective study from 2008 assessing 18 cases of ocular gliomas described an overall incidence of 0.36% for all canine ocular tumors, with 17 astrocytomas and 1 oligodendroglioma (11). Metastatic rate for these tumors is considered low, but 3 cases had evidence of intracranial extension of the tumor (11). Advanced imaging was performed in 2 instances of ocular glioma; however, the published descriptions were limited and images were not made available (9,11). Magnetic resonance imaging (MRI) was done in 1 of these instances (9).

This report describes the progression of a high-grade undefined glioma of the optic nerve in a dog with secondary extension to the brain. The report includes the MRI characteristics and histopathological findings. To the authors' knowledge, this is the first veterinary publication describing an undefined canine intraocular glioma following the release of the revised diagnostic classification of canine glioma (3), and the first detailed report of the MRI findings.

Case description

A 4-year-old neutered male mixed-breed dog (weight: 33.2 kg) was referred to the Small Animal Ophthalmology Service at the Bailey Small Animal Teaching Hospital at Auburn University (Auburn, Alabama) for evaluation of hyphema in the right eye (*oculus dexter,* OD). The dog was initially seen by the referring veterinarian 2 wk earlier for a "red" eye. Intraocular pressure OD was recorded in the medical record as 53 mmHg. At that time, the dog was prescribed a 2-week course of oral doxycycline, oral carprofen, neomycin/polymyxin/dexamethasone ophthalmic ointment, dorzolamide 2%/timolol 0.5%, and latanoprost 0.005% ophthalmic solution, all with undetermined brands, doses, and frequencies. A Fever of Unknown Origin RealPCR Panel (Standard: *Anaplasma* spp., *Babesia* spp., *Bartonella* spp., *Brucella canis, Cryptococcus* spp., *Ehrlichia* spp., *Neospora caninum,* Rocky Mountain spotted fever, *Toxoplasma gondii*) (IDEXX Laboratories, Westbrook, Massachusetts, USA) was submitted, which returned with negative results.

On presentation at Auburn University, the dog was non-visual OD with an absent menace response, absent dazzle reflex, and absent consensual pupillary light reflex of the left eye (*oculus sinister,* OS). The right globe was buphthalmic. Retropulsion of both globes was normal. Due to the dog's excitable nature, sedation with 0.005 mg/kg dexmedetomidine hydrochloride (Dexdormitor 0.5 mg/mL; Zoetis, Parsippany, New Jersey, USA) and 0.4 mg/kg butorphanol tartrate (Torbutrol 10 mg/mL; Zoetis) was administered IM to facilitate the remainder of the ophthalmic examination. Intraocular pressures were measured using rebound tonometry (Icare TonoVet, Vantaa, Finland) with values of 29 mmHg OD and 21 mmHg OS. Slit lamp biomicroscopy (SL-17; Kowa, Tokyo, Japan) was performed for both eyes (*oculus uterque,* OU), revealing conjunctival hyperemia,

chemosis, episcleral injection, deep diffuse corneal edema, and ciliary flush OD. Hyphema filled the anterior chamber OD, obscuring the view of the iris, lens, vitreous body, and fundus. Ophthalmic examination OS, including indirect ophthalmoscopy, was unremarkable. Fluorescein stain was negative OU. Ocular ultrasound (10 mHz ocular ultrasound probe; Aviso, Quantel Medical, Cournon-d'Auvergne, France) OD revealed a hypoechoic vitreal body and complete retinal detachment with multifocal areas of subretinal hyperechoic material. The portion of the retrobulbar structures that could be examined *via* ocular ultrasound were unremarkable. The diagnostic interpretation was panuveitis with hyphema, complete retinal detachment, and secondary glaucoma OD. Differential diagnoses included an infectious etiology, primary ocular neoplasia, metastatic neoplasia, and trauma.

A complete blood (cell) count (CBC) was evaluated and was considered unremarkable. A serum chemistry profile revealed mildly elevated cholesterol (338 mg/dL, reference: 132 to 335 mg/dL), and urinalysis collected by cystocentesis revealed isosthenuria (specific gravity: 1.011) with a quiet sediment, and 3-view thoracic radiographs were normal. An abdominal ultrasound was performed, revealing a diffusely hypoechoic liver and mesenteric, gastric, and portal lymphadenopathy. Aspirates of the liver, spleen, and a mesenteric lymph node were obtained, revealing normal liver and splenic cells and a reactive lymph node. A urine antigen test for Blastomyces (Blastomyces Antigen Enzyme Immunoassay; MiraVista Diagnostics, Indianapolis, Indiana, USA) was taken due to its endemic nature in the respective area, and was negative.

Two days after initial presentation, the dog returned for a subconjunctival enucleation of the right globe. At the time of surgery, no gross abnormalities of the globe and attached optic nerve or the retrobulbar structures were identified. The dog recovered from surgery uneventfully and the globe was submitted for histopathology to the Comparative Ocular Pathology Laboratory (COPLOW) at the University of Wisconsin — Madison.

Grossly, the globe was buphthalmic and had a tan mass overlying the optic nerve head. There was retinal detachment and intraocular hemorrhage (Figure 1 A). Histopathologically, an unencapsulated and entirely necrotic neoplasm infiltrated and expanded the central retina and choroid, projected into the vitreous, and infiltrated the optic nerve to the surgical margin. The necrosis obscured the cellular and architectural details; however, the vasculature of the mass was still prominent. The mass had multiple areas of hemorrhage. Additionally, a robust fibrovascular membrane lined the anterior surface of the iris, crossed the iridocorneal angle, and resulted in anterior synechia and ectropion uveae. The anterior and posterior chambers, vitreous humor, and subretinal space contained varying amounts of hemorrhage. The retina was diffusely detached and atrophied. Based on these findings, a diagnosis of a necrotic optic nerve/retinal glioma with incomplete excision was made. Advanced imaging was discussed with the client but was declined.

The dog returned for a postoperative evaluation 2 wk later. The enucleation site had healed and the complete ophthalmic examination OS, including fundic assessment, was unremarkable.
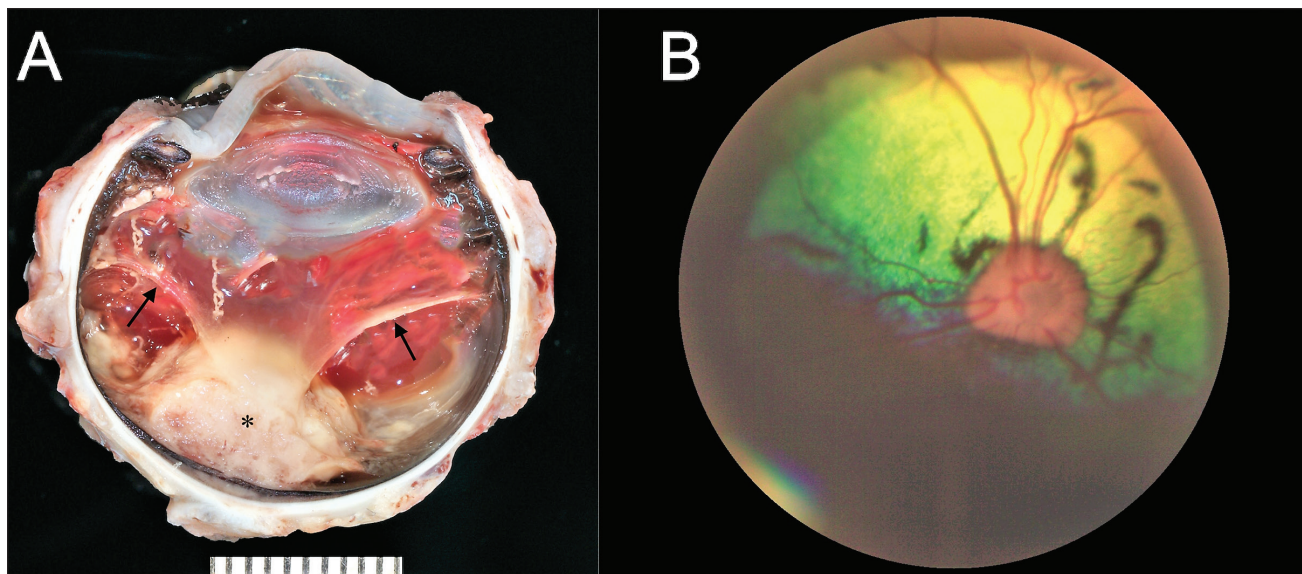
Figure 1. A – Gross image of the sectioned globe of a 4-year-old mixed-breed dog. A tan mass overlies the optic nerve head (*) and retinal detachment is also shown (arrows). Multifocal intraocular hemorrhage is also present. B – Fundic image of the left globe. Multiple peripapillary, dark, vermiform lesions are present in the tapetal fundus.

Eight weeks following enucleation of the right globe, the dog returned for evaluation of the contralateral eye (OS) due to concerns regarding potential discomfort. Ophthalmologic examination OS revealed trace conjunctival hyperemia, a positive menace response, a decreased dazzle reflex, mydriasis, an incomplete direct pupillary light reflex, loss of the physiologic pit of the optic nerve head, and multifocal subretinal linear white infiltrates in the non-tapetal region of the fundus. Intraocular pressure was 11 mmHg using rebound tonometry. Concern for consequences of the contralateral eye secondary to the previously diagnosed neoplasm was considered. The dog was prescribed oral prednisone USP (Novitium Pharma, East Windsor, New Jersey, USA), 0.6 mg/kg, q48h, for undetermined posterior segment changes; dorzolamide HCl 2% ophthalmic solution (Alcon Laboratories, Fort Worth, Texas, USA), OS, q24h, as prophylactic therapy; and neomycin-polymyxin-dexamethasone ointment (Bausch + Lomb, Bridgewater, New Jersey, USA), OS, q12h for 7 d, then q24h for 7 d, for the trace conjunctival hyperemia noted on ophthalmic examination.

Ten weeks following enucleation, the dog was noted to have a depressed mentation but continued to have a positive menace response, positive dazzle reflex, mydriasis, and an incomplete pupillary light reflex OS. Fundic examination revealed resolution of the multifocal subretinal infiltrate; however, multiple peripapillary dark, vermiform lesions were identified in the tapetal region. Images were obtained (Figure 1 B) (ClearView Optical Imaging System; Optibrand, Fort Collins, Colorado, USA). Consultation with a Board-certified veterinary neurologist (TJ) was pursued. Due to the onset of contralateral ocular deficits and a perceived change in patient mentation, MRI of the brain, optic nerves, and left globe was again recommended, but initially declined. The dose of oral prednisone was increased to 1 mg/kg per day for 14 d, then decreased to 0.5 mg/kg per day until the scheduled MRI.

Imaging was eventually carried out at 13 wk after surgery, using a Magnotome Skyra 3T MRI (Siemens Medical Solutions, Malvern, Pennsylvania, USA). Images obtained included T2W, T2-STIR, DWI/ADC, SWI, T2-FLAIR, and pre- and post-contrast T1-MPRAGE images. The primary intracranial lesion was a well-circumscribed, irregularly shaped mass at the level of the optic chiasm causing compression of the 3rd ventricle and rostral portion of the thalamus on the right. This mass was T2 and FLAIR hyperintense (Figure 2), T1 isointense, and absent contrast enhancement. In addition, a large, irregular, multi-lobular mass within the right orbit was noted that contrast enhanced, which was not appreciated clinically (Figure 3). The dog recovered from anesthesia without incident and was discharged with a continued anti-inflammatory course of prednisone for palliative management.

The dog was euthanized 18 wk following the initial diagnosis due to deteriorating quality of life. The left globe and approximately 2 cm of the optic nerve proximal to the globe were removed immediately following euthanasia and submitted to COPLOW for histopathologic evaluation. The remaining tissues were submitted for necropsy to the Department of Pathobiology at Auburn University. The left globe appeared grossly normal. There was multifocal absence of both photoreceptor nuclei and photoreceptor inner and outer segments, with occasional migration of retinal pigmented epithelial cells into the retinal layers. The optic nerve head, optic nerve, and remainder of the globe were unremarkable. No neoplastic cells were identified.

A full necropsy was done within 24 h of euthanasia with routine tissue collection, fixation with 10% neutral-buffered formalin, and routine hematoxylin and eosin (H&E) staining of selected tissues. The remaining tissues revealed a mass in the right orbit and right optic nerve with extension into the diencephalon (Figure 4 A). Histologic features were consistent with a high-grade diffusely infiltrative undefined glioma. The
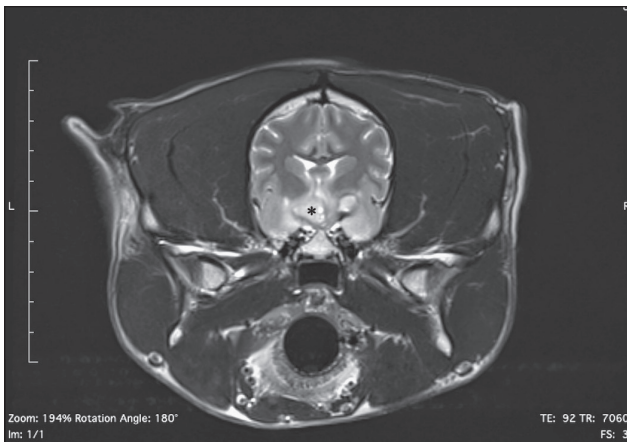
Figure 2. Axial MRI (T2W) imaging in a 4-year-old dog, demonstrating the hyperintense, well-circumscribed, irregularly shaped mass at the level of the optic chiasm causing compression of the 3rd ventricle and rostral portion of the thalamus (*).

Figure 3. Midsagittal T2W MRI image of the same dog showing the same lesion as in Figure 2.

neoplasm was composed of sheets of round-to-polygonal cells, sometimes with lost cytoplasm, within an eosinophilic fibrillary stroma. In addition, the neoplasm had multiple areas of necrosis (Figure 4 B) and rare well-defined, Alcian blue-staining mucinous microcysts (Figure 4 C). At the periphery of the neoplasm, there was nuclear rowing and prominent secondary structure formation, including satellitosis and perivascular aggregates (Figure 4 D). Immunohistochemistry was performed on sections of the diencephalon mass. Neoplastic cells had diffuse and moderate immunoreactivity to oligodendrocyte transcription factor 2 (Olig2, 1:200, ab7260; Abcam, Waltham, Massachusetts, USA) (Figure 5) and lacked immunoreactivity to glial fibrillary acidic protein (GFAP, 1:8000, ab109186; Abcam) and 2′,3′-Cyclic-nucleotide 3′-phosphodiesterase (CNPase, 1:1000, ab6319; Abcam). No neoplastic cells were identified on the section of the left optic nerve. No metastases were evident in other organs.

Discussion

This dog had clinical signs consistent with those reported by Naranjo *et al* for canine ocular gliomas, including hyphema (14/18 globes), glaucoma (10/18 globes), retinal detachment (7/18 globes), and an initial lack of significant ophthalmic findings in the contralateral eye (0/18 cases) (11). A 2018 study by Jinks *et al* showed that, in dogs with hyphema, the most common cause was trauma (26.1%), followed by systemic causes including neoplasia (19.3%), congenital ocular abnormalities (10.2%), immune-mediated thrombocytopenia (9.1%), and systemic hypertension (4.5%). Primary ocular neoplasia was identified in only 5.7% of cases (13). In eyes with hyphema and concurrent retinal detachment for which histopathology was performed (17 eyes), only 4 were diagnosed with ocular neoplasia (13). Although glaucoma does not appear to be specifically associated with ocular neoplasia, 88.2% of eyes with a presenting intraocular pressure above 25 mmHg lost vision during the study (13). Based on this information, localized ocular neoplasia is an uncommon diagnosis when presented with a case of unilateral hyphema, retinal detachment, and glaucoma; however,
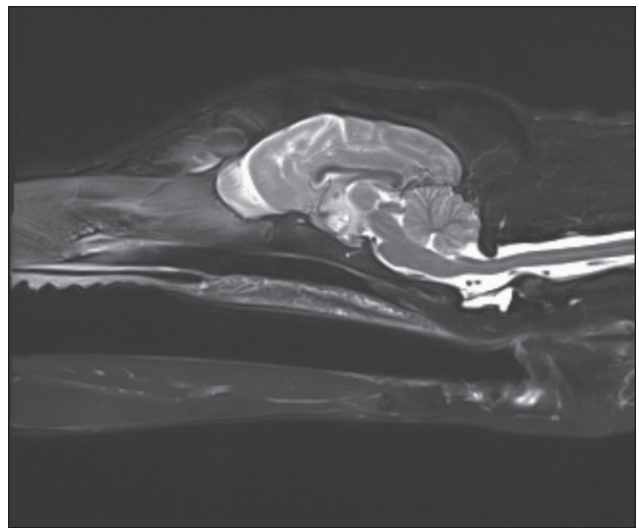
the prognosis for vision can be considered poor, regardless of the inciting cause.

In the present case, based on the presence of clinical ocular signs 2 mo before the development of a depressed mentation and a diminished pupillary light reflex of the left eye, it is anticipated that the tumor originated in the intraocular portion of the optic nerve of the right globe and then extended to and beyond the optic chiasm. This dog's survival period from the time of diagnosis at Auburn University was 18 wk (4.5 mo). In the study by Naranjo *et al,* 8 dogs had neoplastic cells extending to the surgical margin, and survival time did not extend beyond 1 mo for cases that were not lost to follow-up (11). Although this is a limited number of cases to evaluate, long-term survival appears to be poor.

Advanced imaging with MRI was selected because the dog displayed intracranial signs and MRI provides superior soft tissue contrast in the brain. The ocular ultrasound performed with a 10-mHz probe has limitations in its evaluation of the retrobulbar portion of the optic nerve. It is unknown whether the changes in the optic nerve before the time of enucleation could have been identified with more in-depth ultrasound examination.

Notable occurrences in the progression of this case were tumor regrowth in the right orbit and the development of changes in the contralateral globe. The cells in the right orbit had morphology and architecture consistent with the remainder of the right optic nerve and the neoplastic tissue that had extended to the level of the diencephalon. This may reflect the high-grade nature of this tumor resulting in rapid growth. No metastasis was identified on antemortem diagnostics or necropsy. The decreased pupillary light reflex of the left eye (despite apparently functional vision) that was noted at 8 wk following enucleation of the right globe was suspected to be due to intracranial extension of the neoplasm and/or potential involvement of parasympathetic innervation of the oculomotor nerve. No other oculomotor nerve deficits were identified
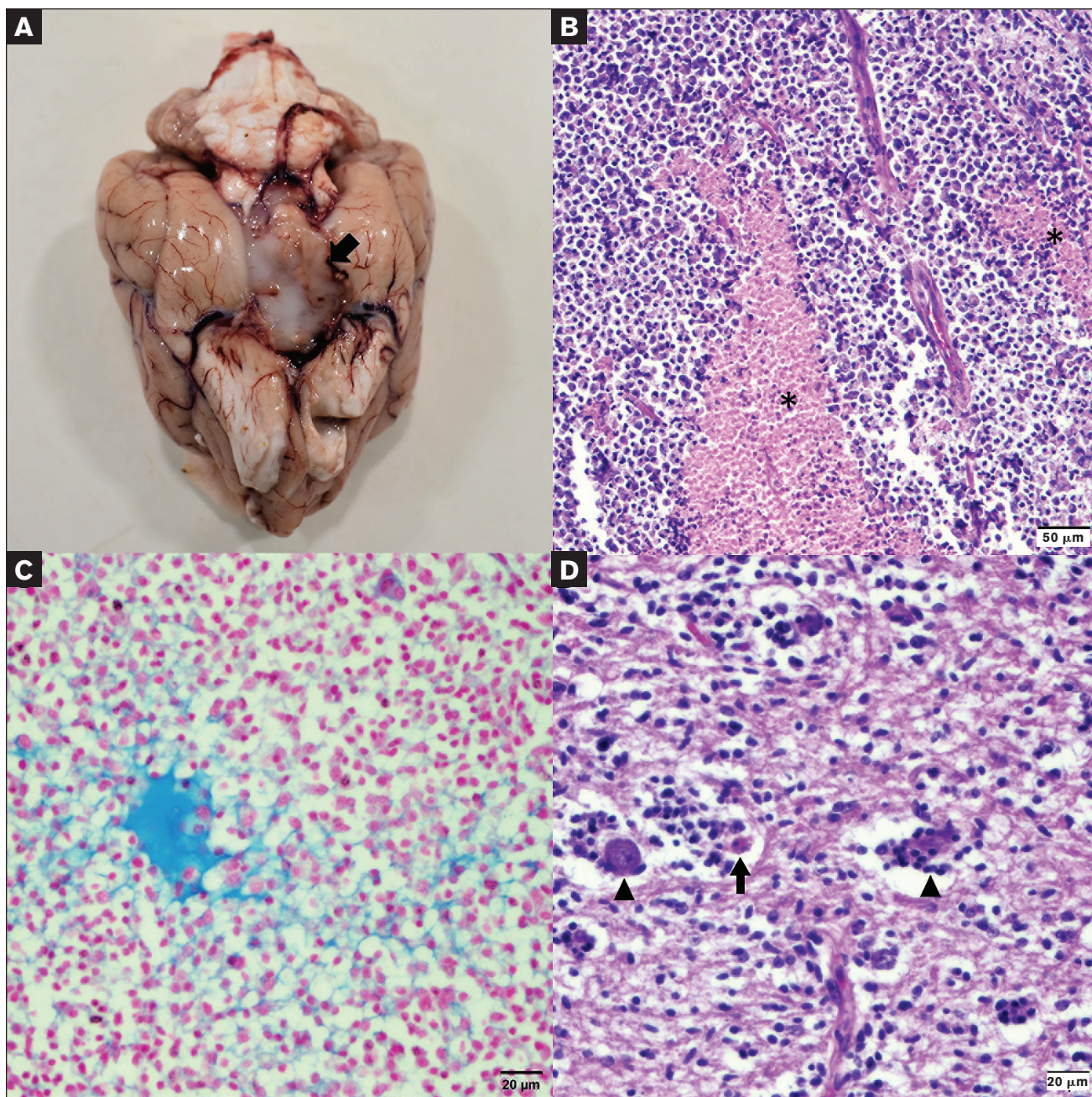
Figure 4. A – Gross photo of the brain of a 4-year-old mixed-breed dog, showing a gelatinous white mass (arrow) invading the diencephalon. B – Hematoxylin and eosin (H&E) histology, 20× magnification. The neoplasm is composed of polygonal cells within an eosinophilic, fibrillary stroma with multifocal areas of necrosis (*). C – Alcian blue histology, 40× magnification. Mucin microcysts within the neoplasm highlight with Alcian blue staining. Mucin microcysts are characteristic of an astrocytic phenotype. D – Hematoxylin and eosin histology, 40× magnification. Neuronal satellitosis (arrowheads) and perivascular aggregates (arrow) form secondary structures, characteristic of an oligodendrocytic phenotype, at the periphery of the neoplasm.

in this dog. Alternatively, the noted retinal changes could have been implicated in a decreased pupillary light reflex, but this was considered unlikely in this case.

The fundic changes of the left eye noted at 8 wk after enucleation of the right globe suggested the possibility of contralateral extension of the neoplasm. The transition from white, linear subretinal infiltrate to dark, vermiform lesions in the tapetal region occurred within 2 wk. Similar changes have been described in dogs with ivermectin toxicity as focal areas of retinal edema (14,15). This consideration was addressed,

and the owners denied any administration of ivermectin or potential access to outdoor areas where exposure to ivermectin could have occurred; however, retinal edema not related to ivermectin administration or ingestion remained possible. Other conditions that can manifest similarly include retinal dysplasia, retinal folds or focal detachments, and linear retinal infiltrate (16). Retinal dysplasia would have been present since birth and noted on previous ophthalmic examinations. Although retinal folds or detachments were a possibility, a "raised" appearance to these structures was not noted. Retinal infiltrate was a
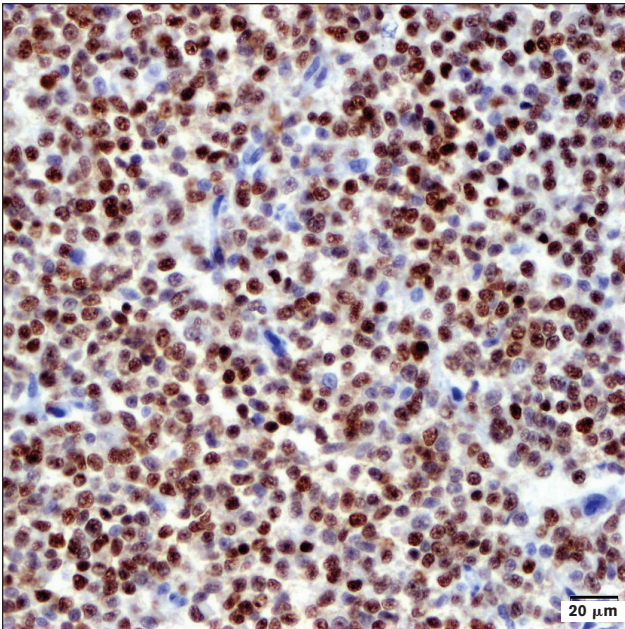
Figure 5. Histology at 40× magnification. Neoplastic cells have strong nuclear immunoreactivity to Olig2, highlighted by 3,3′-diaminobenzidine (DAB) brown chromogen.

differential diagnosis for this finding, as was retinal edema. The dog remained functionally visual until the time of euthanasia.

In similar future cases, an electroretinogram could be considered to evaluate retinal function in the presence of these fundic changes, and optical coherence tomography could be considered to image these regions in greater detail antemortem. Histopathologically, lesions corresponding to the described fundic lesions were difficult to identify; however, areas of photoreceptor nuclei and inner and outer segment loss with occasional migration of retinal pigmented epithelial cells into the retina were noted and may correlate. In the study by Naranjo *et al,* 1 dog that had advanced imaging to identify extension of the tumor to the optic chiasm had a decreased number of ganglion cells in the contralateral eye on histopathology (11). In the present case, the number of ganglion cells in the retina of the left globe was subjectively within normal limits, and the pathogenesis of the development of the vermiform fundic lesions remains speculative at this time.

The current grading and classification system for canine gliomas is based on brain tumor cases and not optic nerve tumors (3). This calls into question if this grading and classification scheme is appropriate for optic nerve gliomas. The tumor was biphenotypic, with histomorphological features of both an astrocytoma and oligodendroglioma, meaning "undefined" is the most appropriate glioma classification. In addition, the decline in the quality of life leading to euthanasia of the dog supports a high-grade tumor. Glial fibrillary acidic protein, including in tumors with clear astrocytic morphology, and CNPase in necropsy tissues are known to have variable immunoreactivity. The most fixation-resistant marker, Olig2, is not a reliable differentiator in dogs between oligodendrocytes and an astrocytic lineage (3). Therefore, the lack of immunoreactivity to GFAP

and CNPase and immunoreactivity to Olig2 in this neoplasm should not dissuade the reader from a diagnosis of undefined glioma.

Although its occurrence is rare, this report emphasizes the validity of maintaining an intraocular glioma as a differential diagnosis for a canine patient presented for unilateral hyphema, glaucoma, and retinal detachment. Advanced imaging of the optic nerves and brain with MRI should be considered in these cases, whether before enucleation if a mass is identified *via* ocular ultrasound, during surgery, or following a histopathologic diagnosis, as intracranial extension may have significant implications for long-term survival.

References

1. Snyder JM, Shofer FS, Van Winkle TJ, Massicotte C. Canine intracranial primary neoplasia: 173 cases (1986–2003). J Vet Intern Med 2006; 20:669–675.
2. Song RB, Vite CH, Bradley CW, Cross JR. Postmortem evaluation of 435 cases of intracranial neoplasia in dogs and relationship of neoplasm with breed, age, and body weight. J Vet Intern Med 2013;27:1143–1152.
3. Koehler JW, Miller AD, Miller CR, *et al.* A revised diagnostic classification of canine glioma: Towards validation of the canine glioma patient as a naturally occurring preclinical model for human glioma. J Neuropathol Exp Neurol 2018;77:1039–1054.
4. Pancotto TE, Rossmeisl JH, Zimmerman K, Robertson JL, Werre SR. Intramedullary spinal cord neoplasia in 53 dogs (1990–2010): Distribution, clinicopathologic characteristics, and clinical behavior. J Vet Intern Med 2013;27:1500–1508.
5. Barnett KC, Grimes TD. Retrobulbar tumour and retinal detachment in a dog. J Small Anim Pract 1972;13:315–319.
6. Spiess BM, Wilcock BP. Glioma of the optic nerve with intraocular and intracranial involvement in a dog. J Comp Pathol 1987;97:79–84.
7. Caswell J, Curtis C, Gibbs B. Astrocytoma arising at the optic disc in a dog. Can Vet J 1999;40:427–428.
8. Martín E, Perez J, Mozos E, Lopéz R, Molleda JM. Retrobulbar anaplastic astrocytoma in a dog: Clinicopathological and ultrasonographic features. J Small Anim Pract 2000;41:354–357.
9. Sisó S, Lorenzo V, Ferrer I, Villagrassa M, Pumarola M. An anaplastic astrocytoma (optic chiasmatic-hypothalamic glioma) in a dog. Vet Pathol 2003;40:567–569.
10. Meyerholz DK, Haynes JS. Solitary retinal astrocytoma in a dog. Vet Pathol 2004;41:177–178.
11. Naranjo C, Schobert C, Dubielzig R. Canine ocular gliomas: A retrospective study. Vet Ophthalmol 2008;11:356–362.
12. Dubielzig RR. Ocular neoplasia in small animals. Vet Clin North Am Small Anim Pract 1990;20:837–848.
13. Jinks MR, Olea-Popelka F, Freeman KS. Causes and outcomes of dogs presenting with hyphema to a referral hospital in Colorado: A retrospective analysis of 99 cases. Vet Ophthalmol 2018;21:160–166.
14. Epstein SE, Hollingsworth SR. Ivermectin-induced blindness treated with intravenous lipid therapy in a dog. J Vet Emerg Crit Care 2013;23: 58–62.
15. Kenny PJ, Vernau KM, Puschner B, Maggs DJ. Retinopathy associated with ivermectin toxicosis in two dogs. J Am Vet Med Assoc 2008; 233:279–284.
16. Ofri R. Diseases of the retina. In: Maggs DJ, Miller PE, Ofri R, eds. Slatter's Fundamentals of Veterinary Ophthalmology. 6th ed. St. Louis, Missouri: Elsevier, 2018:347–389.